Am J Physiol Cell Physiol 283: C1182–C1195, 2002.
First published June 26, 2002; 10.1152/ajpcell.00173.2002.

Cellular and molecular responses to increased skeletal muscle loading after irradiation

GREGORY R. ADAMS,[1] VINCENT J. CAIOZZO,[1,2]
FADIA HADDAD,[1] AND KENNETH M. BALDWIN[1]
Departments of [1]Physiology and Biophysics and [2]Orthopaedics, College of Medicine, University of California, Irvine, California 92697

Received 16 April 2002; accepted in final form 15 June 2002

Adams, Gregory R., Vincent J. Caiozzo, Fadia Haddad, and Kenneth M. Baldwin. Cellular and molecular responses to increased skeletal muscle loading after irradiation. *Am J Physiol Cell Physiol* 283: C1182–C1195, 2002. First published June 26, 2002; 10.1152/ajpcell.00173.2002.—Irradiation of rat skeletal muscles before increased loading has been shown to prevent compensatory hypertrophy for periods of up to 4 wk, possibly by preventing satellite cells from proliferating and providing new myonuclei. Recent work suggested that stem cell populations exist that might allow irradiated muscles to eventually hypertrophy over time. We report that irradiation essentially prevented hypertrophy in rat muscles subjected to 3 mo of functional overload (OL-Ir). The time course and magnitude of changes in cellular and molecular markers of anabolic and myogenic responses were similar in the OL-Ir and the contralateral nonirradiated, overloaded (OL) muscles for the first 3–7 days. These markers then returned to control levels in OL-Ir muscles while remaining elevated in OL muscles. The number of myonuclei and amount of DNA were increased markedly in OL but not OL-Ir muscles. Thus it appears that stem cells were not added to the irradiated muscles in this time period. These data are consistent with the theory that the addition of new myonuclei may be required for compensatory hypertrophy in the rat.

myonuclei; satellite cell

MATURE MAMMALIAN SKELETAL muscle cells are multinucleated myofibers that are formed via the fusion of individual myoblast cells during development. Evidence suggests that these multinucleated myofibers are permanently differentiated and therefore incapable of mitotic activity (8, 21, 54). During muscle regeneration after injury, myofibers can be repaired and/or replaced via the fusion of muscle stem cells (satellite cells) either with existing damaged myofibers or with each other to form new myofibers (43, 48, 49).

The impetus for much of the current interest in the role of satellite cells in muscle adaptation has its roots in the muscle regeneration literature. The results from a number of studies using muscle injury models indicated that relatively modest doses of radiation, well below the threshold of those required to induce overt cellular injury in vivo, interfered with the regeneration of skeletal muscle (see, e.g., Refs. 15, 25, 32). Because there is an absence of overt cellular damage, it was postulated that the failure of myofibers to regenerate resulted from damage to DNA that prevents satellite cell proliferation. It would follow then that mature, permanently differentiated mammalian myofibers would not appear to be the locus of the radiation-induced mitotic failure (8, 54). Thus the inhibitory effects of radiation on muscle regeneration were proposed to be a result of the incapacitation of satellite cell mitotic activity.

The theory that radiation-induced inhibition of cellular proliferation can inhibit mammalian muscle adaptation and repair has recently been extended to include the prevention of compensatory muscle hypertrophy after increased loading. In support of this theory, a number of studies have demonstrated that the muscle hypertrophy process appears to involve the addition of nuclei to existing myofibers (see, e.g., Refs. 44–46, 51) and that prior irradiation can prevent this adaptation (35, 38–41). For example, a series of papers published by Rosenblatt et al. (39–41) showed that, in response to functional overload, irradiated myofibers do not hypertrophy or increase their myonuclear number but do alter their myosin heavy chain (MHC) isoform profile from a faster to a slower phenotype. These results suggest that the irradiated myofibers adapt in a manner similar to that of nonirradiated myofibers with regard to the qualitative expression of contractile protein isoforms but are unable to increase the quantity of protein accumulated in the myofibers. Similarly, Phelan and Gonyea (35) found that after 4 wk of overload, muscle hypertrophy was absent and cell proliferation was significantly less in irradiated vs. control muscles. In addition to the inhibition of either regeneration or hypertrophy, it has also been reported that irradiation prevents the recovery of muscle mass from unloading-induced atrophy in mice (27). In avian muscles, irradiation appears to prevent stretch-induced cellular proliferation, but only a relatively small proportion of the hypertrophy response is affected (26).

Address for reprint requests and other correspondence: G. R. Adams, Dept. of Physiology and Biophysics, Medical Sciences I C308, Univ. of California, Irvine, CA 92697 (E-mail: gradams@UCI.edu).

The costs of publication of this article were defrayed in part by the payment of page charges. The article must therefore be hereby marked "*advertisement*" in accordance with 18 U.S.C. Section 1734 solely to indicate this fact.

Recent reports indicated that there are stem cell populations within skeletal muscle that appear to be resistant to radiation-induced damage (20). In addition, there are data to indicate that stem cells from extramuscular tissues can be incorporated into skeletal muscles, and once there they function as muscle stem cells (12). These results suggest that a pool of mitotically competent stem cells could be available for the eventual restoration of the compensatory hypertrophy response in muscles that have been previously irradiated.

The finding that hypertrophy of mammalian skeletal muscle may require the incorporation of stem cells gives rise to some important hypotheses: *1*) the number of myonuclei present in a muscle fiber is a limiting factor for protein production, indicating that there is not a significant reserve capacity for growth processes dependent on nuclear functions; and *2*) over the time periods studied to date (i.e., up to 4 wk), muscles do not have a source of stem cells other than that which is present in the muscle domain at the time of irradiation.

Therefore, the current study was designed to address portions of these two hypotheses. First we hypothesized that it should be possible to detect and evaluate adaptive responses that involve nuclear function, such as increased RNA levels, generated within myofibers in overloaded-irradiated muscles. Second, we postulated that previous studies may not have allowed sufficient time for either an intrinsic radiation-resistant population of satellite cells or an extramuscular stem cell source to contribute to the development of compensatory hypertrophy. Accordingly, a study was performed with the functional overload model, in which the plantaris muscles were bilaterally overloaded and one leg was then exposed to irradiation while the rest of the animal was protected from the radiation dose. The muscles from subgroups of these rats were studied at specific time points spanning a period of 90 days after treatment.

METHODS

Forty-eight female Sprague-Dawley rats (212 ± 3 g body wt) were randomly assigned to one of eight groups ($n = 6$ per group) for the primary experiments in this study. All procedures were approved by the University of California, Irvine, Institutional Animal Care and Use Committee. In six of these groups one leg was exposed to γ-radiation as follows.

Treatment. In the six groups chosen for treatment, the left hindlimb of the animals was exposed to 25-Gy (2.5 Gy/min) ionizing irradiation with a Mark I irradiator (model 68, J. L. Shepard and Associates, Glendale, CA). The exact dose of irradiation was determined with Fricke dosimetry solution. Irradiation was focused onto the hindlimb of each animal with a collimator, thus allowing the irradiation to be focused onto the hindlimb musculature without exposing the rest of the body. After induction of anesthesia (40 mg/kg ketamine-2 mg/kg acepromazine), the animal was positioned such that the left hindlimb was aligned with the slit of the collimator. Immediately after the irradiation procedure, rats had the plantaris muscles of both legs overloaded via the removal of the gastrocnemius and soleus muscles as described previously (6).

Tissue collection. Groups of rats were killed by injection of Pentosol (Med-Pharmex) at 6 and 24 h and at 3, 7, 15, and 90 days after the irradiation procedure. Two groups of untreated rats were used as controls and were killed at the beginning of the study ($t = 0$) and the end of the 90-day period. On the basis of the results seen in the primary study, additional groups of six rats each were used in a follow-up study to determine whether measurable hypertrophy developed after 4 mo of functional overload.

At the appropriate time point the plantaris muscles of the irradiated and contralateral legs were dissected free of connective tissue, weighed, and snap frozen. Muscles were stored at −80°C for subsequent analysis.

Biochemical and molecular analyses. Tissue samples were analyzed for total DNA and protein content as described previously (1). Myofibrillar protein content was determined via modification of the method described by Solaro et al. (52; see Ref. 57).

Total RNA isolation. Measurements of total RNA content provide insights on the translational capacity of tissue. Total RNA was extracted from preweighed frozen muscle samples with the TRI reagent (Molecular Research Center, Cincinnati, OH) according to the company's protocol, which is based on the method described by Chomczynski and Sacchi (9). Extracted RNA was precipitated from the aqueous phase with isopropanol and, after washing with ethanol, dried and suspended in a known volume of nuclease-free water. The RNA concentration was determined by optical density at 260 nm (using an OD_{260} unit equivalent to 40 μg/ml). The muscle total RNA concentration was calculated based on total RNA yield and the weight of the analyzed sample. The RNA samples were stored frozen at −80°C to be used subsequently in determining both total mRNA (poly A) and specific mRNA expression with slot blotting and relative reverse transcription (RT)-polymerase chain reaction (PCR) procedures.

RNA slot blotting. RNA slot blotting techniques were used to elucidate the contribution of various fractions of RNA to the changes seen in response to treatments. In the current study this analysis was aimed at measuring the total amount of mRNA as well as two markers of contractile protein message. One microgram of total RNA was denatured in twenty microliters of denaturing buffer (18% formaldehyde, 10× SSC) at 60°C for 15 min. Samples were brought up to 100-μl volume with 6× SSC and were applied onto a positively charged nylon membrane (GeneScreen plus; NEN) with a slot blot apparatus (Schleicher and Schuell). Two blot series were performed for each sample. After UV fixation, each membrane was hybridized consecutively with *1*) either an antisense α-skeletal actin mRNA probe to determine α-skeletal actin mRNA expression or an antisense MHC mRNA probe common to all MHC; *2*) an oligo dT probe (12- to 18-mer; Life Technology) that was used to detect poly A RNA (total mRNA population); and *3*) an antisense 18S ribosomal RNA probe. The signal of this probe is directly proportional to the amount of total RNA and thus was used to normalize for possible variability in the amount of loaded RNA per slot. Probes were 5′ end-labeled with ^{32}P with γ-ATP and T4 polynucleotide kinase. Hybridization and washing procedures were carried out as described previously (17). Hybridization signals were detected and analyzed with a phosphorimager and Image Quant analysis software (Molecular Dynamics). The slot blot hybridization signal for these probes was strongly correlated with the amount of loaded total RNA, ranging from 0.25 to 2 μg per slot. For each sample, the MHC mRNA, actin mRNA, and dT (poly A) signals were normal-

ized to the corresponding 18S signal. The mRNA per muscle as reported for MHC and α-skeletal actin mRNA was based on the total RNA content per muscle and the mRNA ratio to 18S.

The sequences of the oligonucleotide probes used for hybridization were as follows: α-skeletal actin antisense probe: GGCTGGCTTTAATGCTTCAAGT (based on reported actin mRNA sequence; GenBank accession no. V01224); MHC antisense probe (common to all rat MHC): TGGTGTCCTGCTCCTTCTT (based on type I MHC mRNA sequence position 5306–5324; GenBank accession no. NM017239; complementary to coding region ~500 nt upstream from stop codon and 100% identical in all MHC isoforms including adult and developmental; signal obtained with this common MHC probe is indicative of total population of MHC mRNA expressed in muscle); 18S rRNA antisense probe: GTGCAGCCCCGGACATCTAAG (based on rat ribosomal RNA sequence; GenBank accession no. M11188).

Reverse transcription. One microgram of total RNA was reverse transcribed for each muscle sample with SuperScript II RT from GIBCO-BRL and a mix of oligo dT (100 ng/reaction) and random primers (200 ng/reaction) in a 20-μl total reaction volume at 45°C for 50 min, according to the provided protocol. At the end of the RT reaction, the tubes were heated at 90°C for 5 min to stop the reaction and then were stored at −80°C until used in the PCR for specific mRNA analyses.

Polymerase chain reaction. A relative RT-PCR method using 18S as an internal standard (Ambion, Austin, TX) was applied to study the expression of specific mRNAs for IGF-I, IGF-I receptor, IGF binding proteins (BP-4 and BP-5), myogenin, cyclin D1, and p21. The sequences for the various primers used for the specific target mRNAs are shown in Table 1. These primers were designed with the Primer Select computer program (DNA Star), purchased from Life Technology GIBCO, and were tested for their compatibility with the alternate 18S primers. It should be noted that for IGF BP-4, the primers' sequence is based on the mouse X76066 sequence. These mouse primers were selected on the basis of regions that are highly similar to the human IGF BP-4 cDNA, and they proved to be effective with rat mRNA. In each PCR reaction, 18S ribosomal RNA was coamplified with the target cDNA (mRNA) to serve as an internal standard and to allow correction for differences in starting amounts of total RNA.

For the 18S amplification we used the alternate 18S internal standards (Ambion), which yield a 324-bp product. The 18S primers were mixed with competimers at an optimized ratio that could range from 1:4 to 1:10, depending on the abundance of the target mRNA. Inclusion of 18S competimers was necessary to bring down the 18S signal, which allows its linear amplification to the same range as the coamplified target mRNA (relative RT-PCR kit protocol; Ambion).

For each specific target mRNA, RT and PCR were carried under identical conditions with the same reagent premix for all the samples to be compared in the study. To validate the consistency of the analysis procedures, at least one representative from each group was included in each RT-PCR run.

One microliter of each RT reaction (0- to 10-fold dilution depending on target mRNA abundance) was used for the PCR amplification. PCR was carried out in the presence of 2 mM $MgCl_2$ with standard PCR buffer (GIBCO), 0.2 mM dNTP, 1 μM specific primer set, 0.5 μM 18S primer-competimer mix, and 0.75 U of DNA *Taq* polymerase (GIBCO) in a total volume of 25 μl. Amplifications were carried out in a Stratagene Robocycler with an initial denaturing step of 3 min at 96°C, followed by 25 cycles of 1 min at 96°C, 1 min at 55°C (55–60°C depending on primers), 1 min at 72°C, and a final step of 3 min at 72°C. PCR products were separated on a 2–2.5% agarose gel by electrophoresis and stained with ethidium bromide, and signal quantification was conducted by laser scanning densitometry, as reported previously (59). In this approach, each specific mRNA signal is normalized to its corresponding 18S. For each primer set, PCR conditions (cDNA dilutions, 18S competimer-primer mix, $MgCl_2$ concentration, and annealing temperature) were set to optimal conditions, so that both the target mRNA and 18S product yields were in the linear range of the semilog plot when the yield is expressed as a function of the number of cycles.

Phosphorylation state of intracellular signaling proteins. The phosphorylation states of the p70-S6 kinase (S6K1) and extracellular signal-regulated kinases 1 and 2 (ERK1/2) were examined by immunoblotting with phosphospecific antibodies (Cell Signaling Technology, Beverly, MA). The antibodies used detected changes in phosphorylation at sites critical for increased activity in vivo (22, 60). Muscle samples were extracted by homogenization in 7 vols of ice-cold *buffer A* [50 mM Tris·HCl, pH 7.8, 2 mM potassium phosphate, 2 mM EDTA, 2 mM EGTA, 50 mM β-glycerophosphate, 10% glyc-

Table 1. *Sequence of specific sets of primers used in RT-PCR mRNA analyses*

Target mRNA	PCR Primer Sequence 5′→3′	Product Size, bp	GenBank Accession No.
IGF-I (all)	5′ sense: GCATTGTGGATGAGTGTTGC	202 all	X06043
	3′ antisense: GGCTCCTCCTACATTCTGTA	254 MGF	
MGF	5′ sense: GCATTGTGGATGAGTGTTGC	163	X06108
	3′ antisense: CTTTTCTTGTGTGTCGATAGG		
IGF-I receptor	5′ sense: CGGCTTCTCTGCAGTAAACACA	245	L29232
	3′ antisense: ACTGGGAAGCGGAGAAAAGAGA		
IGF-BP5	5′ sense: CACGCCTTCGACAGCAGTAAC	214	NM_012817
	3′ antisense: GTCGGGAATGGGGAGTGTCT		
IGF-BP4	5′ sense: CCTGGGCTTGGGGATGC	212	X76066
	3′ antisense: AGGGGTTGAAGCTGTTGTTGG		
Myogenin	5′ sense: ACTACCCACCGTCCATTCAC	233	M24393
	3′ antisense: TCGGGGCACTCACTGTCTCT		
Cyclin D	5′ sense: AAGTGCGTGCAGAGGGAGAT	267	D14014
	3′ antisense: GGGGCGGATAGAGTTGTCAG		
p21	5′ sense: CCCGTGGACAGTGAGCAGTT	233	U24174
	3′ antisense: AGCAGGGCCGAGGAGGTA		

RT, reverse transcription; PCR, polymerase chain reaction; MGF, mechanosensitive IGF-I isoform.

erol, 1% Triton X-100, 1 mM DTT, 3 mM benzamidine, 1 mM sodium orthovanadate, 10 μM leupeptin, 5 μg/ml aprotinin, 200 μg/ml soybean trypsin inhibitor, and 1 mM 4-(2-aminoethyl)benzenesulfonyl fluoride (AEBSF)] with a motor-driven glass pestle. The homogenate was immediately centrifuged at 12,000 *g* for 30 min at 4°C. The supernatant was immediately saved in aliquots at −80°C for subsequent use in immunoblotting. The supernatant protein concentration was determined by using the Bio-Rad protein assay with BSA as the standard. Approximately 50 μg of supernatant proteins were subjected to sodium dodecyl sulfate-polyacrylamide gel electrophoresis (SDS-PAGE; 12.5% T), according to a standard protocol (24), and then electrophoretically transferred to a polyvinylidene difluoride (PVDF) membrane (Immobilon-P) with 10% methanol, 1 mM orthovanadate, 25 mM Tris, and 193 mM glycine, pH 8.3. Phospho-ERK1/2 and phospho-S6K1 were detected with phosphorylation state-specific antibodies (Cell Signaling Technology) and an enhanced chemiluminescence (ECL) method of detection (Amersham). Signal intensity was determined by laser scanning densitometry (Image Quant; Molecular Dynamics). For each specific antibody, all the samples were run under identical (previously optimized) conditions, including the transfer on the membrane, the reaction with the first and secondary antibodies, washing conditions, ECL detection, and the film exposure. To ensure the consistency of this analysis, at least one representative sample from each group was included in each gel run and Western blot analysis. In addition, a positive control, provided by the antibody supplier, was run on each gel to allow for normalization. For each set of Western blotting and detection conditions, the detected signal was directly proportional to the amount of protein loaded on the gel over a 20- to 150-μg range (data not shown).

Confocal microscopy for determination of cell volumes and myonuclei number. At the time of death, an ~5-mm segment was taken from the midbelly of each muscle and frozen in isopentane that was cooled by liquid nitrogen. Subsequently, the muscle sample was thawed as described by Allen et al. (4), and single fibers segments (n ≈ 10 fiber segments/muscle) were isolated by placing the muscle sample in a small dissection chamber containing a glycerol-relaxing solution (50% glycerol, 2 mM EGTA, 1 mM $MgCl_2$, 4 mM ATP, 10 mM imidazole, 100 mM KCl, pH 7.0). Dissection was performed with a microscope (Technival 2, Jena, Germany) with back lighting and microsurgical forceps (super fine Dumont tweezers; Biomedical Research Instruments, Rockville, MD). Isolated fiber segments were placed into a PBS solution containing Hoechst 33258, a DNA binding agent that acquires specific excitation/emission spectrum properties on DNA binding and thus can be used to image the nuclei with fluorescence microscopy (Molecular Probes, Eugene, OR). The fiber segment was then washed several times in PBS and then placed into a PBS solution containing BODIPY-labeled phallicidin (Biomolecular Probes). Phallicidin binds selectively to actin and serves as a tool for identifying the dimensions of the fiber. After these labeling procedures, the fiber segment was washed in PBS and mounted on a glass slide with glycerol. The coverslip had struts to prevent compression of the muscle fiber segment when it was mounted. The volume of a muscle fiber segment, its length, and the corresponding number of myonuclei were determined with a MRC 600 Bio-Rad laser scanning confocal microscope and a magnification of ×400. The images were then reconstructed and rendered with Advanced Visualization Software version 6.0 (AVS; Waltham, MA). By using the volume integration module of AVS, it was possible to determine the volume of the single-fiber segment. This approach allows the expression of myonuclei distribution relative to length (nuclei/mm) and volume (μm^3/nuclei). All measurements of muscle fiber segment length and volume were normalized to a sarcomere length of 2.5 μm. This sarcomere length was chosen because this was the value observed by us in other studies in our laboratories examining the architecture of the plantaris muscle (unpublished observations; $n \approx$ 24,000 measurements of sarcomere length).

MHC isoform analysis. A portion of each muscle sample was homogenized in a solution that contained (in mM) 250 sucrose, 100 KCl, 5 EDTA, and 10 Tris-base. The homogenate protein was diluted to 1 mg/ml in a storage buffer containing 50% glycerol, 100 mM $Na_4P_20_7$, 5 mM EDTA, and 2 mM 2-mercaptoethanol (pH 8.8) and stored at −20°C until subsequent analyses for MHC protein content.

Skeletal MHCs were separated with a SDS-PAGE technique. The method used is a modification of that published by Talmadge and Roy (55), which allows for the detection of all six rat MHC isoforms (3). The separating gel contained 30% glycerol, 8% acrylamide, 1.5 M Tris-base, 1 M glycine, and 10% SDS. The stacking gel contained 4% acrylamide, 30% glycerol, 0.5 M Tris·HCl, 100 mM EDTA, and 0.4% SDS. Protein samples were denatured by placing 5 μg of sample in 35 μl of sample buffer and heating the solution for 2 min at 100°C. The sample buffer consisted of 5% β-mercaptoethanol, 100 mM Tris-base, 5% glycerol, 4% SDS, and bromophenol blue. The gels were run at 275 V for ~22 h under refrigeration. The gels were stained with Brilliant Blue G 250 (Sigma) and destained, and then they were scanned and quantified with a Molecular Dynamics densitometer (Sunnyvale, CA). The peaks of interest representing the distinct MHC isoforms were identified in the digitized densitometric data sets. The area of each peak was determined by integration and was indicative of the relative expression of the corresponding MHC isoform.

Statistical analysis. All values are reported as means ± SE. For each time point, treatment effects were determined by ANOVA with post hoc testing [Student-Newman-Keuls (SNK)] with the Prism software package (Graphpad). Pearson correlation analysis was used to assess the relationship between myofibrillar protein and DNA and between p21 and myogenin with the Prism package. For all statistical tests the 0.05 level of confidence was accepted for statistical significance.

RESULTS

At the end of 3 mo after irradiation, the body weight of the γ-radiation-treated rats was not different from that of the untreated control group [305 ± 5 and 318 ± 6 g, respectively (synergist ablation removes ~4 g of muscle)]. This result indicates that the localized irradiation did not have any adverse effects on the generalized growth of the treated animals (initial body wt 212 ± 3 g). In addition, pilot data indicated that the myofibrillar yield, cross-sectional area (CSA), and force production of irradiated muscles were not altered relative to controls 4 wk after this irradiation protocol was imposed (data not shown).

Muscle hypertrophy. Fifteen days of overload resulted in significant muscle hypertrophy in non-irradiated overloaded (OL) muscles as evidenced by increased muscle mass (Fig. 1*A*). Ninety days of overload resulted in further hypertrophy (Fig. 1). In the overloaded muscles that were irradiated (OL-Ir), there was

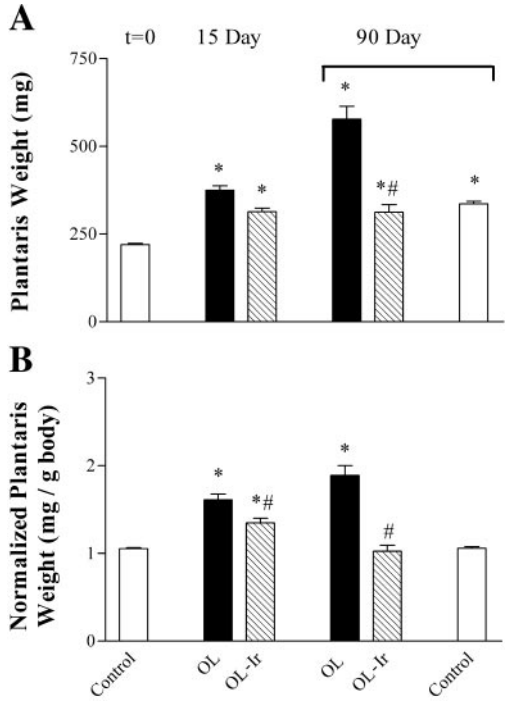

Fig. 1. *A*: removal of synergists results in a substantial increase in plantaris muscle wet weight in nonirradiated (OL) muscles. A small but significant hypertrophy response was detected in the overloaded-irradiated (OL-Ir) muscles at 15 days, with no further increase in mass over 90 days of overload treatment. The mass of the plantaris muscles from control rats increased as a result of growth such that the absolute weight of the muscles of the 90-day control group was significantly larger than that from the rats killed at the beginning of the study (time $t = 0$). *B*: when normalized for body weight increases, the plantaris wet weight of the 90-day OL-Ir muscles and the 90-day control muscles was not different than that of the $t = 0$ control rats. $^{*}P < 0.05$ vs. $t = 0$; $^{\#}P < 0.05$ vs. OL (contralateral muscle).

a small increase in mass at both 15 and 90 days after treatment relative to the $t = 0$ normal control muscles. When normalized to body mass, the observed changes in mass in the OL-Ir group at 90 days were no longer significant (Fig. 1*B*). In addition, the 90-day values for the OL-Ir muscles were not different from those of the 90-day untreated controls (Fig. 1). Similar results were seen for the total muscle protein content (data not shown).

Myofibrillar protein was used as a conservative marker of hypertrophic adaptation to avoid the potential complications of acute inflammatory response that may occur with this treatment during the first 3–5 days (5). The myofibrillar protein content of the OL plantaris muscles was significantly increased at 7 (27%), 15 (57%) and 90 (2.6-fold) days after surgery compared with the zero time point control muscles (Fig. 2). In contrast, the OL-Ir muscles demonstrated only a transient increase at the 24 h time point (Fig. 2). The young adult female rats used in this study continued to increase body mass (+50%) over the 3-mo period of this study. As a result, some portion of the observed myofibrillar protein increase was most likely related to this generalized growth process. For example, compared with the 90-day control, the increase in 90-day

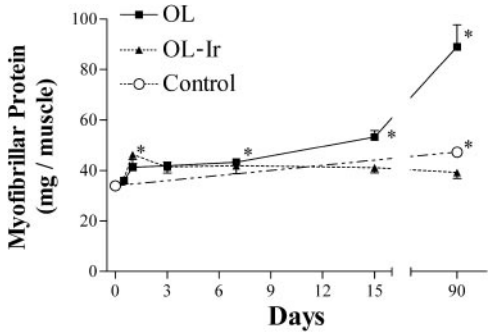

Fig. 2. Myofibrillar protein content of the OL muscles was progressively increased by 7, 15, and 90 days of overload treatment. A small increase in myofibrillar protein in the OL-Ir muscles was evident after 1 day of increased loading. The myofibrillar protein content of the 90-day control rats was higher than that of the $t = 0$ controls. $^{*}P < 0.05$ vs. $t = 0$.

OL muscle myofibrillar protein was 1.8-fold as opposed to a 2.6-fold increase compared with the $t = 0$ controls (Fig. 2).

The myofibrillar protein content of the OL-Ir muscles at 90 days was not different from that of untreated muscles of animals in the 90-day control group. However, the myofibrillar protein content of the 90-day control muscles had increased ~40% compared with the $t = 0$ controls (Fig. 2). This suggests that the myofibrillar protein content of the OL-Ir muscles remained proportional to the amount of body growth seen over the 90 days.

Cell proliferation. The DNA content of both OL and OL-Ir muscles was increased at 15 and 90 days after treatment compared with the $t = 0$ control group (Fig. 3). However, the increase in DNA content seen in the OL-Ir muscles was smaller than that in the OL group. The DNA content of the OL-Ir group was not different from that seen in the 90-day controls. In both OL and OL-Ir muscles, the concentration of DNA (e.g., in mg/g) was unchanged over time (data not shown). This finding demonstrates the apparent coordination

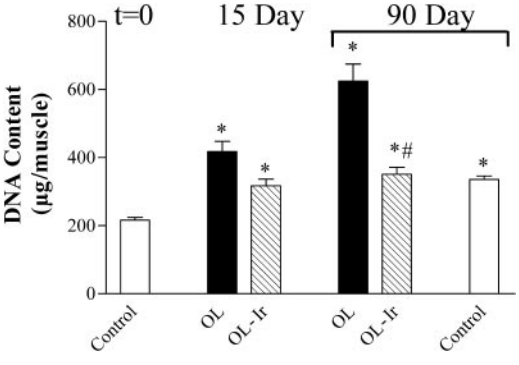

Fig. 3. Overload stimulus resulted in a significant increase in DNA content in the OL muscles. A small but significant increase in DNA content was also seen in OL-Ir muscles at 15 days, with no further increase in DNA detected over the remainder of the 90-day overload treatment. DNA content of the plantaris muscles from control rats was increased at 90 days. There were no changes in DNA concentration in any muscles (data not shown). $^{*}P < 0.05$ vs. $t = 0$; $^{\#}P < 0.05$ vs. OL.

of DNA and cell size in both growing and hypertrophying muscles.

Over the course of this study, the relationship between DNA and myofibrillar protein content followed a similar pattern in the OL and OL-Ir groups (Fig. 4*A*). Consistent with the possibility of an early inflammatory response (5), there was a small increase in DNA at the early time points after the ablation surgery in both groups. Despite this early complication, the overall relationship between DNA and myofibrillar protein resulted in a strong correlation in the OL muscles (Fig. 4*B*). In contrast, the early increases in DNA in the OL-Ir muscles were not paralleled by increased myofibrillar protein and hence did not show a significant correlation (data not shown). Figure 4*A* is essentially a combination of the data presented in Figs. 2 and 3. Thus it is particularly striking to note that the large increase in DNA content (Fig. 3) seen in the OL muscles is associated with an increase in myofibrillar protein (Fig. 2) such that the ratio of these two variables is the same as that seen for the control groups at 90 days (Fig. 4*A*).

Myonuclear analysis. CSA and myonuclear number were determined in single fibers from $t = 0$ and 90-day plantaris muscles. CSA of myofibers from the OL muscles was significantly increased (46%) at 90 days after overload (Fig. 5*A*). There was no change in the CSA of myofibers from OL-Ir muscles. The number of myonuclei per millimeter of myofiber length was significantly increased in myofibers from the OL (44%) but not the OL-Ir plantaris muscles (Fig. 5*B*). As a result of the increase in myonuclei in the OL muscles, the myofiber volume-to-myonucleus ratio remained unchanged (Fig. 5*C*).

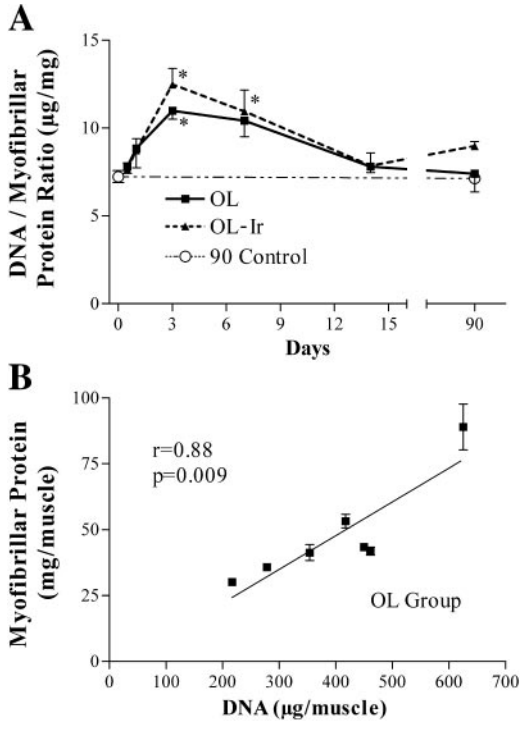

Fig. 4. *A*: ratio of DNA to myofibrillar content changed with a similar pattern in both OL and OL-Ir plantaris muscles. There was no change in this ratio in the muscles from control rats. *B*: there was a significant correlation between myofibrillar protein and DNA content in the OL but not the OL-Ir plantaris muscles. $^{*}P < 0.05$ vs. $t = 0$.

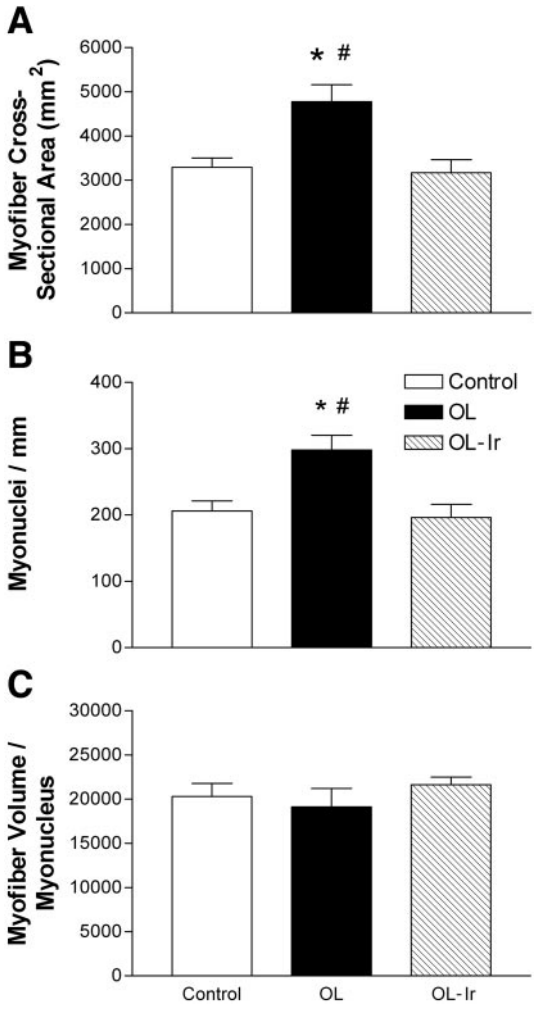

Fig. 5. *A*: overload resulted in a significant increase in the cross-sectional area of OL but not OL-Ir plantaris muscle fibers. *B*: there was an increase in no. of myonuclei per millimeter of myofiber in the OL but not OL-Ir myofibers. *C*: ratio of the myofiber volume per myonucleus was unchanged in both the treatment and control groups. $^{*}P < 0.05$ vs. $t = 0$; $^{\#}P < 0.05$ vs. contralateral OL-Ir.

Cellular signaling response to increased loading. The phosphorylation state of both S6K1 and 4E binding protein 1 (4E-BP1) was markedly increased at very early time points after the imposition of increased loading in both OL and OL-Ir muscles (Fig. 6). In the OL muscles, phosphorylation of 4E-BP1 and S6K1 remained elevated through the 15-day time point and returned to control levels by 90 days. In the OL-Ir muscles, the increase in phosphorylation of these proteins appeared to be resolved by the 7 day time point (Fig. 6).

The phosphorylation of both ERK1 and -2 was increased at very early time points after the initiation of overloading in both OL and OL-Ir muscles (Fig. 7). By

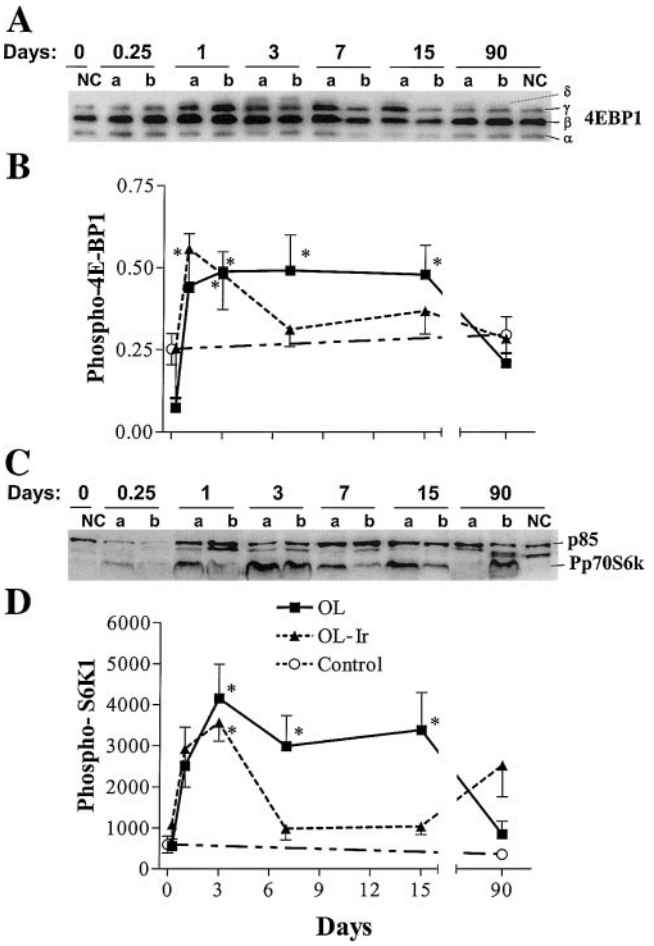

Fig. 6. Phosphorylation state of the inhibitory eukaryotic initiation factor 4E binding protein (4E-BP1; *A* and *B*) and of p70 S6 kinase (S6K1; *C* and *D*) was increased in both OL and OL-Ir plantaris muscles at early time points. Phosphorylation state of 4E-BP1 and of S6K1 in the OL and OL-Ir muscles diverged after 3 days. There was no change in 4E-BP1 or S6K1 phosphorylation state in the muscles from control rats (○). *A* and *C* are representative Western blot images for 4E-BP1 and phospho-S6K1, respectively. Phosphorylation state for 4E-BP1 represents the ratio between slow-migrating isoforms (δ and γ) and faster-migrating forms (α and β) (13). NC, normal control; a, OL; b, OL-Ir. $^*P < 0.05$ vs. $t = 0$.

7 days after treatment, the phosphorylation levels of the ERKs had returned to or below the baseline values.

Molecular marker responses to increased loading. The amount of total RNA per muscle increased in both OL and OL-Ir muscles through 7 days of increased loading (Fig. 8*A*). This value remained elevated in the OL muscles through 90 days, whereas in the OL-Ir muscles it returned to baseline between the 7 and 15 day time points.

A similar pattern was seen for total mRNA, which remained elevated through 90 days in the OL muscles but declined to control levels by 15 days in the OL-Ir muscles (Fig. 8*B*). The proportion of mRNA to total RNA as determined by dT-to-18S ratio was essentially unchanged during the course of the study (data not shown).

The expression of the mRNA for the mechanosensitive isoform of IGF-I (MGF; Ref. 18) was significantly upregulated at 1 and 3 days after treatment and then declined toward baseline values in both OL and OL-Ir muscles (Fig. 9). Other components of IGF-I-related systems also changed in a similar pattern in both OL and OL-IR muscles. Similar to our previous reports (2, 16), overloading significantly increased the expression of IGF-I mRNA by 24 h of treatment, returning to baseline values between the 15 and 90 day time points (data not shown). The increase in IGF-I mRNA was similar for OL and OL-Ir muscles. The mRNA for the type 1 IGF-I receptor was significantly increased only at the 1 day time point in both OL and OL-Ir muscles (data not shown). The mRNA for IGF BP-5 was unchanged, whereas that for IGF BP-4 was increased similarly in OL and OL-Ir muscles at 3 and 7 days of increased loading (data not shown).

The expression of the mRNA for the myogenic regulatory factor myogenin was significantly elevated to a very similar degree at 24 and 72 h after the overloading surgery in OL and OL-Ir muscles (Fig. 10). The expression of this mRNA declined to baseline in both muscles at 15 days but was again significantly increased at 90 days in the OL-Ir muscles but not the OL muscles. The pattern of changes seen in the expression of MGF and myogenin appeared to be quite similar.

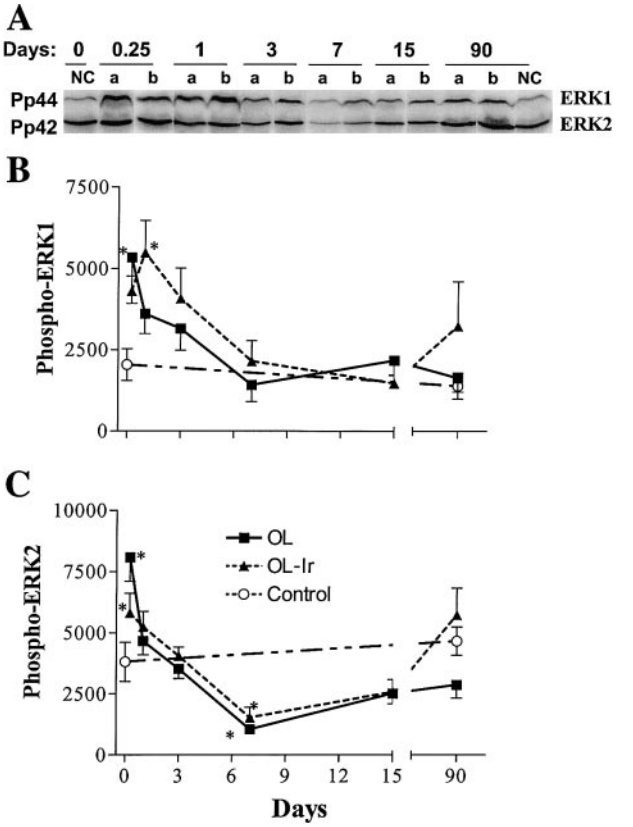

Fig. 7. *A*: representative Western blot image for phospho-extracellular signal-regulated kinase (ERK)1/2 detection. Both ERK1 (p44) and ERK2 (p42) are detected with the same phosphospecific antibody. Phosphorylation state of ERK1 (*B*) and -2 (*C*) was increased in both OL and OL-Ir plantaris muscles at very early time points, then declined in parallel. There was no change in ERK1 and -2 phosphorylation state in the muscles from control rats. $^*P < 0.05$ vs. $t = 0$.

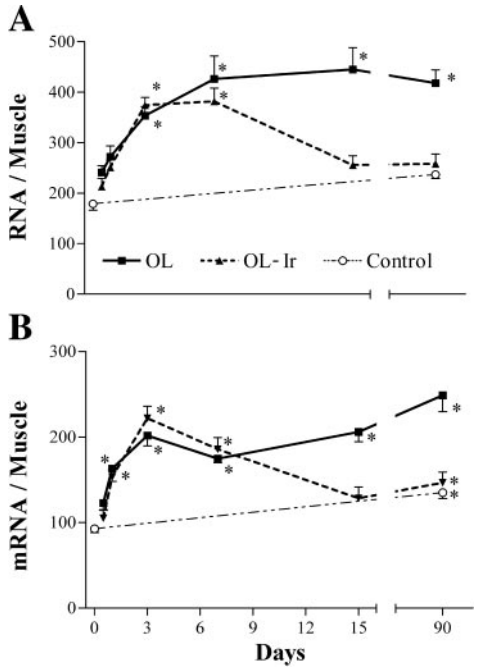

Fig. 8. Total RNA (*A*) and total mRNA (*B*) per muscle were significantly increased in both OL and OL-Ir plantaris muscles until the 7 day time point. Both RNA and mRNA remained significantly elevated through 90 days in OL but not OL-Ir muscles. There was a significant increase in total mRNA but not total RNA at 90 days in the muscles from control rats. *$P < 0.05$ vs. $t = 0$. *x*-Axes in arbitrary scan units.

Increased expression of cyclin D1 and the cyclin-dependent kinase inhibitor (CKI) p21 are indicative of cells either entering into the cell cycle (cyclin D1) or exiting from the cell cycle (p21). The expression of cyclin D1 mRNA increased significantly in both OL and OL-Ir muscles, indicating that a population of cells within the muscles was preparing to become mitotically active (Fig. 11). The increase in cyclin D1 was much greater in the OL-Ir muscles than in the OL muscles at all time points. For example, at 3 days the cyclin D1 mRNA was increased approximately threefold and fivefold in OL and OL-Ir muscles, respectively. Cyclin D1 mRNA remained elevated in the OL-Ir muscles throughout the 90 days of the study. In the OL muscles, cyclin D1 mRNA tended to be increased, but this change (vs. $t = 0$) was significant only at 1 and 3 days after treatment (Fig. 11).

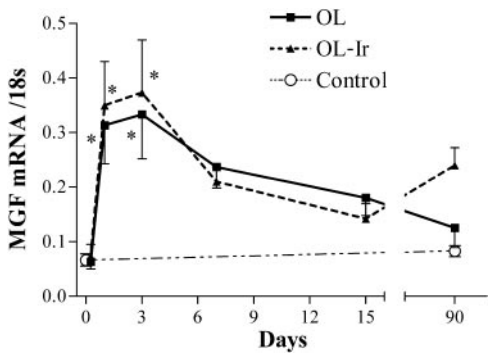

Fig. 9. mRNA for mechanosensitive growth factor (MGF) was significantly increased in both OL and OL-Ir plantaris muscles until the 3 day time point, then declined toward baseline. There was no change in MGF mRNA in the muscles from control rats. *$P < 0.05$ vs. $t = 0$.

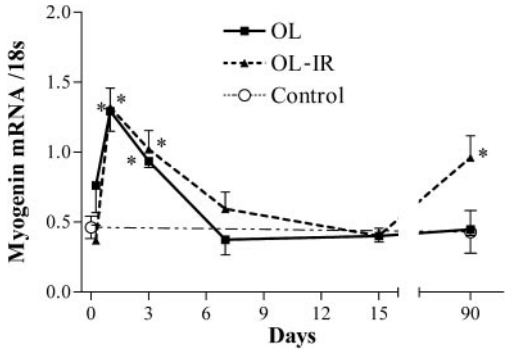

Fig. 10. mRNA for the myogenic regulatory factor myogenin was significantly increased in both OL and OL-Ir plantaris muscles until the 3 day time point, then declined toward baseline. Myogenin mRNA was significantly increased at 90 days in the OL-Ir muscles. There was no change in myogenin mRNA in the muscles from control rats. *$P < 0.05$ vs. $t = 0$.

The expression of p21 mRNA was increased at very early time points in both OL and OL-Ir muscles (Fig. 12). However, there was a much greater increase in p21 mRNA expression in OL-Ir than in OL muscles. As we previously reported (2, 16) there was a significant correlation ($r = 0.77$, $P = 0.04$) between the increased expression of p21 mRNA and myogenin mRNA in OL but not OL-Ir muscles.

The expression of actin and MHC mRNA were used to assess contractile protein-specific molecular responses to increased loading. The amount of MHC mRNA in the OL-Ir muscles did not increase relative to $t = 0$ values and was significantly lower at 90 days compared with the 90-day control muscles. The amount of MHC mRNA per OL muscle was significantly increased after the 15 day time point (Fig. 13*A*). In contrast, the amount of actin mRNA present in muscles increased at earlier time points and remained elevated over the 90-day course of this study in OL but not OL-Ir muscles (Fig. 13*B*).

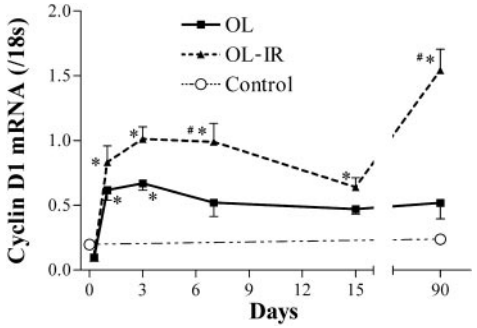

Fig. 11. mRNA for the cell cycle regulator cyclin D1 was significantly and similarly increased in both OL and OL-Ir plantaris muscles until the 3 day time point. Cyclin D1 mRNA remained elevated throughout the 90-day overload period in the OL-Ir but not the OL muscles. There was no change in cyclin D1 mRNA in the muscles from control rats. *$P < 0.05$ vs. $t = 0$; #$P < 0.05$ vs. OL.

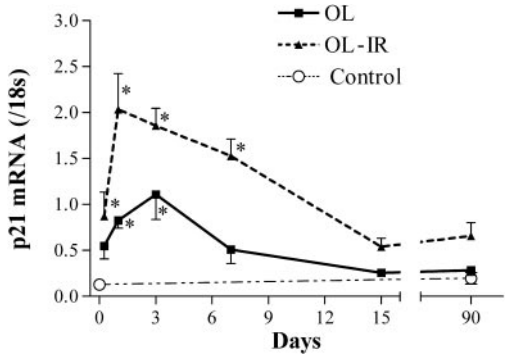

Fig. 12. mRNA for the cyclin-dependent kinase inhibitor p21 was significantly increased through 3 and 7 days in OL and OL-Ir plantaris muscles, respectively. Increase in p21 D1 mRNA in the OL-Ir muscles was greater than that seen in OL muscles at most time points. There was no change in cyclin D1 mRNA in the muscles from control rats. *$P < 0.05$ vs. $t = 0$.

MHC isoforms. Increased mechanical loading of the plantaris resulted in the classic fast-to-slow shift in MHC protein expression in both OL and OL-Ir muscles (Fig. 14). This pattern of adaptation appeared to be accentuated in the OL-Ir muscles. For example, the type I MHC isoform, representing the slowest phenotype, represented <5% of the total MHC pool in control rat plantaris muscles. In the OL-Ir muscles, this isoform was increased more than eightfold to 20% of the total MHC present. Similarly, the IIb MHC expression declined by 62% in OL muscles and 80% in OL-Ir muscles. As a result of the exaggerated adaptation of the OL-Ir muscles, ~50% of the MHC present was either type I or IIa, whereas these isoforms represented only ~25% of the MHC in the OL muscles.

DISCUSSION

Irradiation has been used for some time in studies of skeletal muscle regeneration and compensatory growth. Originally, this modality was used to block skeletal muscle regeneration after injury. The interpretation of the results of these various studies has been predicated on the notion that the lasting effects of the radiation treatment were those associated with chromosomal damage (e.g., double strand breaks, cross-linking, base pair loss, etc). It is commonly assumed that the primary outcome of this treatment involves the prevention of mitotic activity within the affected muscles.

More recently, a number of studies have demonstrated that irradiation also appears to prevent skeletal muscle hypertrophy in rats (21, 35, 39–41). However, these studies were conducted before reports that *1*) identified a population of stem cells that are apparently resistant to radiation-induced damage (20) and *2*) found that stem cells from extramuscular tissues can be incorporated into skeletal muscles (12). Because the cited irradiation studies were carried out over a relatively short time span (4 wk), they did not rule out the possibility that extramuscular and/or radiation-resistant stem cells might eventually contribute to the development of compensatory hypertrophy given a longer overload stimulus. The results of the current study extend the period for postirradiation overloading to 3 mo. In that extended period, the hypertrophy response was negligible in the OL-Ir muscles.

Prevention of hypertrophy is not absolute. At the 15 day time point there was a small but significant increase in the mass and myofibrillar protein content of the OL-Ir plantaris muscles (Figs. 1 and 2). During this time period, the DNA content of the OL-Ir muscles also increased by a small but significant amount (Fig. 3). This suggests the possibility that a small number of satellite cells or myogenic precursor cells (MPC) within the irradiated muscles may have been able to complete mitosis. These cells may have been undamaged by the irradiation treatment or have been able to affect repairs to their DNA (29). Alternatively, there may have been a small population of unfused satellite cells or MPCs that responded to the overload stimulus via differentiation and fusion with myofibers. In support of this second alternative, in a study with finer temporal resolution, we found (2) that the increase in expression of p21 and myogenin mRNA precedes that of cyclin D1 in response to increased loading and thus may signal the presence of such a cell population. Over the remainder of the 3-mo course of this study, the myofibrillar protein content of the OL-Ir muscles remained essentially constant, e.g., they did not experience the large increase in myofibrillar protein accumulation seen in the OL muscles (Fig. 2). Assuming that normal

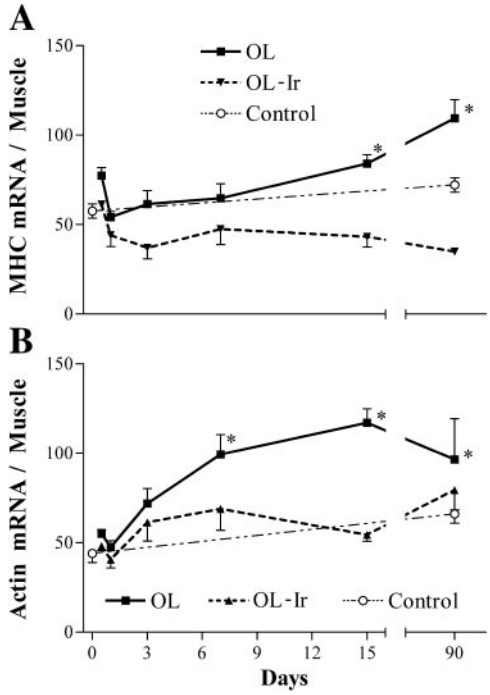

Fig. 13. *A*: mRNA for myosin heavy chain (MHC) (probe common to all rat isoforms) was significantly increased in OL plantaris muscles at both 15 and 90 days. There were no significant changes in MHC mRNA in the muscles from OL-Ir or control rats. *B*: mRNA for α-skeletal actin was significantly increased in OL plantaris muscles at 7, 15, and 90 days. There were no significant changes in α-actin mRNA in the muscles from OL-Ir or control rats. *$P < 0.05$ vs. $t = 0$. *x*-Axes in arbitrary scan units.

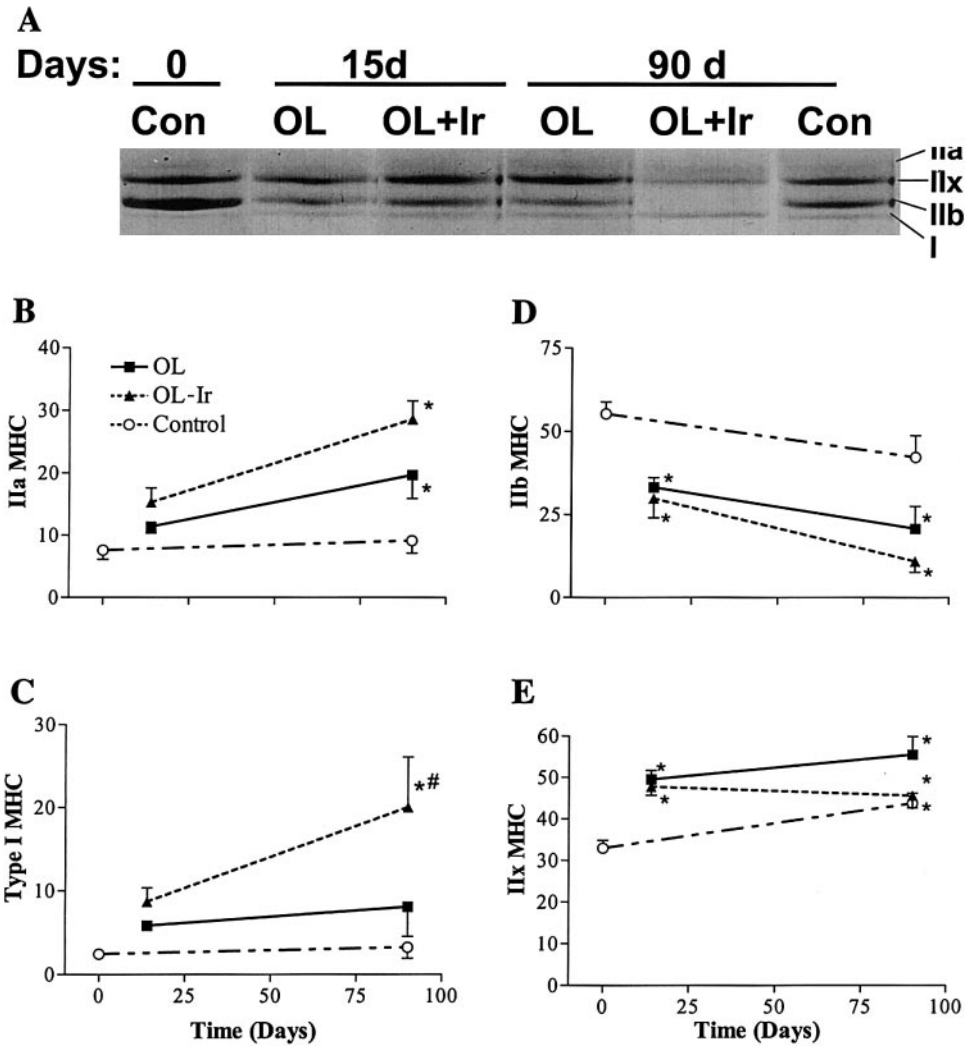

Fig. 14. *A*: representative gel image for MHC isoform separation. Proportion (% of total) of MHC protein isoforms present in OL and OL-Ir plantaris muscles changed significantly over the 90-day treatment period. *B*: type IIa MHC increased significantly in both OL and OL-Ir muscles. *C*: type I MHC increased significantly in OL-Ir but not OL muscles. *D*: decrease in expression of MHC IIb in both OL and OL-Ir muscles was significant at both the 15 and 90 day time points. *E*: type IIx MHC increased in both muscle treatment groups and was significant at both 15 and 90 days. In the muscles from control rats, the only significant change was an increase in type IIx MHC at 90 days. $^{*}P < 0.05$ vs. $t = 0$; $^{\#}P < 0.05$ vs. OL.

cycles of protein turnover continued, these results suggest that the housekeeping mode of transcription and translation was unimpaired by the irradiation treatment. The small increase in myofibrillar protein seen in the early stages of the OL-Ir treatment also suggests that the myofibers had the capacity not only to renew components of the contractile machinery but also to implement a growth and/or limited hypertrophy program. In addition, the current data would suggest that the inhibition of the hypertrophy response was not related to the production of muscle-specific mRNAs, such as that for MHC, because the conversion from fast to slow MHC expression was robust in the irradiated muscles. In contrast to the OL-Ir muscles, the contralateral OL muscles demonstrated a continuous compensatory hypertrophy response detectable from 7 days onward (Fig. 2).

Differential responses to overload. Examination of the data from the first 3–7 days of overload in this study suggests that the responses of the OL and OL-Ir muscles were not different. The first significant divergence in response between these two treatments can be seen in what arguably might be the most temporally sensitive measurements, the increased phosphorylation of S6K1 and 4E-BP1. Increases in the phosphorylation of S6K1 and 4E-BP1 have been reported to be associated with an increase in translation and are known to occur in response to *1*) increased muscle loading and/or *2*) IGF-I receptor ligation (10, 11, 13, 23, 34, 62). The activation of S6K1 has a relatively modest positive impact on translation in general, but, more importantly, it increases the translation of specific mRNAs that encode components of the translational apparatus itself (19, 56). Phosphorylation of 4E-BP1 results in its dissociation from the eukaryotic initiation factor (eIF)4G binding site on eIF4E, allowing for the formation of the translation initiation complex and thereby increasing translation (53). At 3 days after treatment the phosphorylation of S6K1 was increased more than sixfold in both OL and OL-Ir muscles. However, at 7 days, when phospho-S6K1 was increased fivefold in the OL muscles, it was not different from control in OL-Ir muscles. Subsequent to this response, other parameters demonstrated similarly dramatic divergence. For example, at 7 days after treatment total RNA was increased approximately twofold in both OL

and OL-Ir muscles. At 15 days, the RNA of the OL muscles was still increased more than twofold, whereas the RNA content of the OL-Ir muscles had essentially returned to baseline. The total RNA pool primarily reflects the amount of ribosomal RNA present and thus is indicative of the translational capacity of the tissue. Similar to the total RNA pool, the total mRNA present in both sets of muscles was increased at early time points and then diverged between 7 and 15 days. Interestingly, the changes in specific mRNA expression did not demonstrate this pattern of abrupt divergence. In each case there was no difference (e.g., MGF and myogenin), a greater excursion (e.g., cyclin D1 and p21), or a lack of response (e.g., actin and MHC) in the OL-Ir muscles.

The observation of correlations between increased myogenin and p21 expression suggests that the process of satellite cell differentiation is underway in overloaded skeletal muscles (2). In the current study the increase in expression of myogenin was similar in OL and OL-Ir muscles. However, the increase in p21 mRNA levels was much greater in the OL-Ir muscles and did not correlate with the changes in myogenin. In general, the CKI p21 is thought to participate in the initiation of the differentiation process. Because it did not appear that the OL-Ir muscles were increasing their complement of DNA (and therefore cell number), the increase in differentiation signaling appears to be a paradox. However, in this instance the greatly increased p21 expression may be unrelated to the overloading stimulus. For example, there is evidence that cellular responses to radiation-induced DNA damage include withdrawal from the cell cycle to institute repair processes (see, e.g., Ref. 31). This process is mediated by p53, which is upstream from p21. Therefore, the increase in p21 expression seen in the OL-Ir muscles may reflect periods during which mechanisms involved in attempts at chromosomal repair are active rather than processes involved in muscle hypertrophy.

An additional point of divergence in the response to increased loading is evident in the expression of MHC proteins (Fig. 14). The exaggerated shift to slower MHC expression in the OL-Ir muscles represents a compensatory adaptation most likely stimulated by the inability of these muscles to increase their mass or CSA. This shift would provide for greater energetic economy as the overloaded muscles cope with the demands of increased loading.

The data from this study suggest several mechanistically important conclusions. First, the initial ability of the OL-Ir muscles to respond appropriately to the increase in loading state indicates that the cellular systems associated with anabolic processes (e.g., increased translation and transcription) were probably not damaged by the irradiation treatment. Second, the myonuclei of the OL-Ir muscles continued to participate in the adaptation process via the shift in MHC protein expression.

Unfortunately, the methods used in this study do not allow for the differentiation of responses that would be purely anabolic from those that were promoting attempts at cellular proliferation. For example, increased protein production within myofibers is probably reflected by the increase in total RNA as more ribosomes are produced to meet the demand for translation. However, ribosomal synthesis would also be expected to increase markedly in cells that are becoming mitotically active (see, e.g., Ref. 61). Similarly, activation of the pathways including S6K1 activation would also be critical for both anabolic processes and cellular proliferation (19, 23). As a result, it is difficult to speculate on the mechanisms underlying the observed divergence responses in the OL vs. OL-Ir muscles. However, it seems clear that some regulatory processes acted to downregulate cellular responses in the OL-Ir muscles in the 3- to 15-day time frame. It is possible that this is simply a result of the aborted mitotic processes in the incapacitated stem cell populations. However, the magnitude of the changes (e.g., doubling of the RNA content; a 6- to 7-fold increase in phospho-S6K1) suggests that a significant portion of this activity was occurring in the myofibers because these cells represent the majority of the tissue mass. This conclusion is supported by the cyclin D1 and p21 mRNA data (Figs. 11 and 12), which indicate that stem cells within the OL-Ir muscles were continually attempting to enter the cell cycle throughout the study period. These cells would be expected to have elevated levels of growth-promoting signals and components; however, the OL-Ir data do not reflect a substantial contribution from this cell population (e.g., mostly baseline values). This lack of contribution from muscle stem cells agrees with results of previous studies such as that published by Phelan and Gonyea (35) in which the incorporation of bromodeoxyuridine, a marker of mitotic activity, was greatly increased in OL but not OL-Ir muscles.

Role of muscle stem cells. The premise that the failure of stem cells to provide nuclei to myofibers is the primary lesion imposed by the irradiation treatment implies that some processes related to myonuclear function are limiting for the development of hypertrophy. In the case of injury-regeneration studies, the necessity for mitotic activity is relatively clear; muscle cells are destroyed by toxins or mechanical damage and therefore must be replaced by the de novo development of myotubes via the proliferation, differentiation, and fusion of muscle stem cells (satellite cells and/or MPCs). However, in the context of skeletal muscle compensatory hypertrophy, the requirement for mitotic activity is less obvious. If, in fact, the fusion of newly made myoblasts with existing myofibers is required for the hypertrophy response, then this would suggest that a number of nuclear processes were already functioning at or near maximal capacity in the existing myofibers before the increase in loading. This raises a number of intriguing questions. The most obvious of these questions is what specific processes, mediated by myonuclei, actually limit the development of myofiber hypertrophy. Second, why does a lack of newly formed myonuclei more or less permanently prevent hypertrophy rather than just slowing the pro-

cess? For example, in the rat synergist ablation model, the absolute stimulus for the hypertrophic response is essentially continuous, whereas the relative stimulus declines as the muscle enlarges. Logic would suggest that in response to this stimulus, the existing mechanisms for fiber hypertrophy would remain activated until the stimulus for adaptation declines. However, in irradiated muscles, this does not appear to be the case. The various markers of anabolism, such as enhanced translation initiation (e.g., S6K1 and 4E-BP1) or increased translational capacity (e.g., total RNA) initially respond appropriately but then return to baseline levels even though the overload stimulus apparently continues.

Nuclear function and hypertrophy. The results of this study appear to support the hypothesis that the irradiation protocol inhibits compensatory hypertrophy via the prevention of cell proliferation, ultimately depriving the myofibers of their needed reserve for expansion of the myonuclear pool. If this is the case, then an examination of potential mechanisms for this result is warranted.

One of the primary limitations imposed by the bulk amount of DNA present in a given myofiber is the ability to produce the apparatus for mRNA translation (28). Although protein production via mRNA is subject to potential amplification via multiple translations by ribosomes, rRNA and tRNA are the final gene products; thus mass production requires many DNA templates (14, 28). As reviewed by Booth et al. (7), there is evidence that a general increase in translational efficiency occurs at the onset of muscle hypertrophy. However, sustained increases in protein production appear to require substantial increases in the translational machinery. For example, in the hypertrophying heart, early adaptations include an increase in translational efficiency and an acceleration of the synthesis of new ribosomes (30, 50). In multinucleated myofibers, current dogma suggests that the number of copies of rRNA and tRNA genes can only be manipulated via changes in the number of nuclei present.

There is evidence that higher volumes of transcriptional activity will require an increase in space within the nucleus (14). Thus it is possible that the physical spacing within the myonuclei may become a limiting factor during times of high transcriptional activity. If the dense packing of macromolecules within myofibers restricts the expansion of nuclear volume, then it is possible that the addition of satellite cells and their nuclei to myofibers might allow for the distribution of transcriptional loads, thus surmounting this obstacle. However, a number of reports indicate that the RNA produced by a myonucleus may have a fairly limited range of distribution within a myofiber (33, 37, 36). This would suggest that differential transcription requiring mRNA translocation to other myonuclear domains might not be an option for dealing with nuclear space restrictions.

As a general rule, slow myofibers are thought to have a greater number of myonuclei per millimeter and a lower cytoplasm volume-to-myonucleus ratio than fast myofibers (21, 47). In particular, the difference in cytoplasm volume-to-myonucleus ratio between fast and slow fibers in mixed fast muscles, such as the rat plantaris, is fairly pronounced (42, 58). It would therefore follow that the OL-Ir muscles from the current study might have been expected to have a decreased cytoplasm volume-to-myonucleus ratio compared with the controls. However, despite a substantial shift toward slower MHC expression, the whole muscle DNA concentration and single-fiber cytoplasmic volume-to-myonucleus ratio of the OL-Ir muscles were unchanged from controls. This suggests that the lower cytoplasmic volume-to-myonucleus ratio seen in slow fibers may not be a necessary condition for the expression of the type I MHC isoform.

Potential for adaptation after 3 mo. The data from the OL-Ir muscles indicated a tendency toward an upswing at 90 days for a number of measurements (Figs. 4*A*, 6*B*, 7, and 11–13). In the case of myogenin and cyclin D1 mRNA, these increases were significant compared with the $t = 0$ control values. This suggested that these muscles might be entering a new phase of potentially anabolic activity that could lead to a much delayed hypertrophy response. Accordingly, an additional cohort of rats was subjected to OL-Ir protocol to allow for an additional month (i.e., total of 4 mo) for the development of muscle hypertrophy. At 4 mo we observed no indication of a hypertrophic response (e.g., no increase in muscle mass) in the OL-Ir muscles of these rats. Although these 4-mo observations demonstrate that the increases in some cellular and molecular markers at 3 mo did not herald the delayed onset of a compensatory hypertrophy response, they did not shed any light on the reason for these increases.

In summary, the results of this study demonstrate that irradiation essentially prevents the development of compensatory hypertrophy in rodent skeletal muscles for up to 4 mo. This would suggest that neither endogenous or extramuscular stem cells contribute significantly to the stem cell population of overloaded muscles, at least in this time frame. Localized irradiation protocols do not appear to induce significant damage to myofibers or the intrinsic mechanisms necessary for them to adapt to increased loading. The results of this study tend to support the hypothesis that the mechanisms by which myofibers adapt to increased loading appear to include an obligatory "myogenic" component involving the proliferation, differentiation, and fusion of muscle stem cells with the existing myofibers.

The authors thank Anqi Qin, Ming Zeng, Sam McCue, and Mike Baker for invaluable technical assistance.

This work was supported by National Space Biomedical Research Institute Grant NCC9-58 (K. M. Baldwin) and National Institute of Arthritis and Musculoskeletal and Skin Diseases Grants AR-45594 (G. R. Adams) and AR-46856 (V. J. Caiozzo).

REFERENCES

1. **Adams GR and Haddad F.** The relationships between IGF-1, DNA content, and protein accumulation during skeletal muscle hypertrophy. *J Appl Physiol* 81: 2509–2516, 1996.

2. **Adams GR, Haddad F, and Baldwin KM.** Time course of changes in markers of myogenesis in overloaded rat skeletal muscles. *J Appl Physiol* 87: 1705–1712, 1999.
3. **Adams GR, Haddad F, McCue SA, Bodell PW, Zeng M, Qin A, Qin X, and Baldwin KM.** Effects of spaceflight and thyroid deficiency on rat hindlimb development. II. Expression of MHC isoforms. *J Appl Physiol* 88: 904–916, 2000.
4. **Allen DL, Monke SR, Talmadge RJ, Roy RR, and Edgerton VR.** Plasticity of myonuclear number in hypertrophied and atrophied mammalian skeletal muscle fibers. *J Appl Physiol* 78: 1969–1976, 1995.
5. **Armstrong RB, Marum P, Tullson P, and Saubert CW.** Acute hypertrophic response of skeletal muscle to removal of synergists. *J Appl Physiol* 46: 835–842, 1979.
6. **Baldwin KM, Valdez V, Herrick RE, MacIntosh AM, and Roy RR.** Biochemical properties of overloaded fast twitch skeletal muscle. *J Appl Physiol* 52: 467–472, 1982.
7. **Booth FW, Tseng BS, Fluck M, and Carson JA.** Molecular and cellular adaptation of muscle in response to physical training. *Acta Physiol Scand* 162: 343–350, 1998.
8. **Chambers RL and McDermott JC.** Molecular basis of skeletal muscle regeneration. *Can J Appl Physiol* 21: 155–184, 1996.
9. **Chomczynski P and Sacchi N.** Single-step method of RNA isolation by acid guanidinium thiocyanate-phenol-chloroform extraction. *Anal Biochem* 162: 156–159, 1987.
10. **Dufner A and Thomas G.** Ribosomal S6 kinase signaling and the control of translation. *Exp Cell Res* 253: 100–109, 1999.
11. **Farrell PA, Hernandez JM, Fedele MJ, Vary TC, Kimball SR, and Jefferson LS.** Eukaryotic initiation factors and protein synthesis after resistance exercise in rats. *J Appl Physiol* 88: 1036–1042, 2000.
12. **Ferrari G, Cusells-De Angelis G, Coletta M, Paolucci E, Stornaiuolo A, Cossu G, and Mavilio F.** Muscle regeneration by bone marrow-derived myogenic progenitors. *Science* 279: 1528–1530, 1998.
13. **Gingras AC, Kennedy SG, O'Leary MA, Sonenberg N, and Hay N.** 4E-BP1, a repressor of mRNA translation, is phosphorylated and inactivated by the Akt(PKB) signaling pathway. *Genes Dev* 12: 502–513, 1998.
14. **Gregory TR.** Coincidence, coevolution, or causation? DNA content, cell size, and the C-value enigma. *Biol Rev Camb Philos Soc* 76: 65–101, 2001.
15. **Gulati AK.** The effect of X-irradiation on skeletal muscle regeneration in the adult rat. *J Neurol Sci* 78: 111–120, 1987.
16. **Haddad F and Adams GR.** Acute cellular and molecular responses to resistance exercise. *J Appl Physiol* 93: 394–403, 2002.
17. **Haddad F, Herrick RE, Adams GR, and Baldwin KM.** Myosin heavy chain expression in rodent skeletal muscle: effects of zero gravity. *J Appl Physiol* 75: 2471–2477, 1993.
18. **Hameed M, Harridge SDR, and Goldspink G.** Sarcopenia and hypertrophy: a role for insulin-like growth factor-1 in aged muscle? *Exerc Sport Sci Rev* 30: 15–19, 2002.
19. **Hashemolhosseini S, Nagamine Y, Morley SJ, Desrivières S, Mercep L, and Ferrari S.** Rapamycin inhibition of the G_1 to S transition is mediated by effects on cyclin D1 mRNA and protein stability. *J Biol Chem* 273: 14424–14429, 1998.
20. **Heslop L, Morgan JE, and Partridge TA.** Evidence for a myogenic stem cell that is exhausted in dystrophic muscle. *J Cell Sci* 113: 2299–2308, 2000.
21. **Hughes SM and Schiaffino S.** Control of muscle fiber size: a crucial factor in ageing. *Acta Physiol Scand* 167: 307–312, 1999.
22. **Karin M.** The regulation of AP-1 activity by mitogen-activated protein kinases. *Philos Trans R Soc Lond B Biol Sci* 351: 127–134, 1996.
23. **Kawasome H, Papst P, Webb S, Keller GM, Johnson GL, and Gelfand EW.** Targeted disruption of p70s6k defines its role in protein synthesis and rapamycin sensitivity. *Proc Natl Acad Sci USA* 95: 5033–5038, 1998.
24. **Laemmli UK.** Cleavage of structural proteins during the assembly of the head of bacteriophage T4. *Nature* 227: 680–685, 1970.
25. **Lewis RB.** Changes in striated muscle following single intense doses of X-rays. *Lab Invest* 3: 48–55, 1954.
26. **Lowe DA and Alway SE.** Stretch-induced myogenin, MyoD, and MRF4 expression and acute hypertrophy in quail slow-tonic muscle are not dependent upon satellite cell proliferation. *Cell Tissue Res* 296: 531–539, 1999.
27. **Mitchell PO and Pavlath GK.** A muscle precursor cell-dependent pathway contributes to muscle growth after atrophy. *Am J Physiol Cell Physiol* 281: C1706–C1715, 2001.
28. **Montagne J.** Genetic and molecular mechanisms of cell size control. *Mol Cell Biol Res Commun* 4: 195–202, 2000.
29. **Mozdziak PE, Schultz E, and Cassens RG.** The effect of in vivo and in vitro irradiation (25 Gy) on the subsequent in vitro growth of satellite cells. *Cell Tissue Res* 283: 203–208, 1996.
30. **Nagatomo Y, Carabello BA, Hamawaki M, Nemoto S, Matsuo T, and McDermott PJ.** Translational mechanisms accelerate the rate of protein synthesis during canine pressure-overload hypertrophy. *Am J Physiol Heart Circ Physiol* 277: H2176–H2184, 1999.
31. **Niibe Y, Nakano T, Ohno T, Tsujii H, and Oka K.** Relationship between p21/WAF-1/CIP-1 and apoptosis in cervical cancer during radiation therapy. *Int J Radiat Oncol Biol Phys* 44: 297–303, 1999.
32. **Pagel CN and Partridge TA.** Covert persistence of mdx mouse myopathy is revealed by acute and chronic effects of irradiation. *J Neurol Sci* 164: 103–116, 1999.
33. **Pavlath GK, Rich K, Webster SG, and Blau HM.** Localization of muscle gene products in nuclear domains. *Nature* 337: 570–573, 1989.
34. **Petley T, Graff K, Jiang W, and Florini J.** Variation among cell types in the signaling pathways by which IGF-I stimulates specific cellular responses. *Horm Metab Res* 31: 70–76, 1999.
35. **Phelan JN and Gonyea WJ.** Effect of radiation on satellite cell activity and protein expression in overloaded mammalian skeletal muscle. *Anat Rec* 247: 179–188, 1997.
36. **Ralston E and Hall ZW.** Restricted distribution of mRNA produced from a single nucleus in hybrid myotubes. *J Cell Biol* 119: 1063–1068, 1992.
37. **Ralston E, McLaren RS, and Horowitz JA.** Nuclear domains in skeletal myotubes: the localization of transferrin receptor mRNA is independent of its half-life and restricted by binding to ribosomes. *Exp Cell Res* 236: 453–462, 1997.
38. **Robertson TA, Grounds MD, and Papadimitriou JM.** Elucidation of aspects of murine skeletal muscle regeneration using local and whole body irradiation. *J Anat* 181: 265–276, 1992.
39. **Rosenblatt DJ and Parry DJ.** Gamma irradiation prevents compensatory hypertrophy of overloaded mouse extensor digitorum longus muscle. *J Appl Physiol* 73: 2538–2543, 1992.
40. **Rosenblatt JD and Parry DJ.** Adaptation of rat extensor digitorum longus muscle to gamma irradiation and overload. *Pflügers Arch* 423: 255–264, 1993.
41. **Rosenblatt JD, Yong D, and Parry DJ.** Satellite cell activity is required for hypertrophy of overloaded adult rat skeletal muscle. *Muscle Nerve* 17: 608–613, 1994.
42. **Roy RR, Monke SR, Allen DL, and Edgerton VR.** Modulation of myonuclear number in functionally overloaded and exercised rat plantaris fibers. *J Appl Physiol* 87: 634–642, 1999.
43. **Sabourin LA and Rudnicki MA.** The molecular regulation of myogenesis. *Clin Genet* 57: 16–25, 2000.
44. **Salleo A, LaSpada G, Falzea G, Denaro MG, and Cicciarello R.** Response of satellite cells and muscle fibers to long-term compensatory hypertrophy. *J Submicrosc Cytol Pathol* 15: 929–940, 1983.
45. **Schiaffino S, Bormioli SP, and Aloisi M.** Cell proliferation in rat skeletal muscle during early stages of compensatory hypertrophy. *Virchows Arch B Cell Pathol* 11: 268–273, 1972.
46. **Schiaffino S, Bormioli SP, and Aloisi M.** The fate of newly formed satellite cells during compensatory muscle hypertrophy. *Virchows Arch B Cell Pathol* 21: 113–118, 1976.
47. **Schmalbruch H and Lewis DM.** Dynamics of nuclei of muscle fibers and connective tissue cells in normal and denervated rat muscles. *Muscle Nerve* 23: 617–626, 2000.
48. **Schultz E.** Satellite cell behavior during skeletal muscle growth and regeneration. *Med Sci Sports Exerc* 21: S181–S186, 1989.
49. **Schultz E and McCormick KM.** Skeletal muscle satellite cells. *Rev Physiol Biochem Pharmacol* 123: 213–257, 1994.

50. **Siehl D, Chua BH, Lautensack-Belser N, and Morgan HE.** Faster protein and ribosome synthesis in thyroxine-induced hypertrophy of rat heart. *Am J Physiol Cell Physiol* 248: C309–C319, 1985.
51. **Snow MH.** Satellite cell response in rat soleus muscle undergoing hypertrophy due to surgical ablation of synergists. *Anat Rec* 227: 437–446, 1990.
52. **Solaro RJ, Pang DC, and Briggs FN.** The purification of cardiac myofibrils with Triton X-100. *Biochim Biophys Acta* 245: 259–262, 1971.
53. **Sonnenberg N and Ginggras AC.** The mRNA 5′ cap-binding protein eIF4E and control of cell growth. *Curr Opin Cell Biol* 10: 268–275, 1998.
54. **Stockdale FE and Holtzer H.** DNA synthesis and myogenesis. *Exp Cell Res* 24: 508–520, 1961.
55. **Talmadge RJ and Roy RR.** Electrophoretic separation of rat skeletal muscle myosin heavy-chain isoforms. *J Appl Physiol* 75: 2337–2340, 1993.
56. **Thomas G and Hall MN.** TOR signaling and control of cell growth. *Curr Opin Cell Biol* 9: 782–787, 1997.
57. **Thomason DB, Herrick RE, and Baldwin KM.** Activity influences on soleus muscle myosin during rodent hindlimb suspension. *J Appl Physiol* 63: 138–144, 1987.
58. **Tseng BS, Kasper CE, and Edgerton VR.** Cytoplasm to myonucleus ratios and succinate dehydrogenase activities in adult rat slow and fast muscle fibers. *Cell Tissue Res* 275: 39–49, 1994.
59. **Wright C, Haddad F, Qin A, and Baldwin KM.** Analysis of myosin heavy chain mRNA expression by RT-PCR. *J Appl Physiol* 83: 1389–1396, 1997.
60. **Yau L, Lukes H, McDiarmid H, Werner J, and Zahradka P.** Insulin-like growth factor-I (IGF-I)-dependent activation of pp42/44 mitogen-activated protein kinase occurs independently of IGF-I receptor kinase activation and IRS-1 tyrosine phosphorylation. *Eur J Biochem* 266: 1147–1157, 1999.
61. **Zahradka P, Larson DE, and Sells BH.** Regulation of ribosome biogenesis in differentiated rat myotubes. *Mol Cell Biochem* 104: 189–194, 1991.
62. **Zheng Z, Messi ML, and Delbono O.** Age-dependent IGF-1 regulation of gene transcription of Ca^{2+} channels in skeletal muscle. *Mech Ageing Dev* 122: 373–384, 2001.